Wideband and wide-view circular polarizer for a transflective vertical alignment liquid crystal display

Je-Wook Moon,[1] Wan-Seok Kang,[1] Hag yong Han,[1] Sung Min Kim,[2] Seung Hee Lee,[2,3] Yong gyu Jang,[4] Chul Heon Lee,[5] and Gi-Dong Lee[1,*]

[1]Department of Electronics Engineering, Dong-A University, Busan 604-714, South Korea

[2]Polymer BIN Fusion Research Center, Department of Polymer Nano Science and Technology, Chonbuk National University, Chonju, Chonbuk 561-765, South Korea

[3]lsh1@chonbuk.ac.kr

[4]Samsung Mobile Display Co., Ltd., Sungsung-dong, Cheonan, Chungnam 331-300, South Korea

[5]Department of Electronics, Busan College of Information Technology, Busan 616-737, South Korea

*Corresponding authors: gdlee@dau.ac.kr

Received 2 April 2010; revised 4 June 2010; accepted 7 June 2010; posted 11 June 2010 (Doc. ID 126416); published 5 July 2010

We propose an optical configuration for a transflective mode with a circular polarizer for the vertical alignment liquid crystal cell, which can show the wideband property of high contrast in oblique incidence. The proposed configuration consists of a biaxial film and two uniaxial films for satisfying both the transmissive and the reflective modes. Optimization of the optical configuration of the circular polarizer has been performed on the Poincaré sphere in the entire visible wavelength range using the Stokes vector and the Mueller matrix method. We also verify the excellent optical characteristics of the proposed configuration by comparing the viewing angle and contrast ratio in the oblique direction with a conventional optical configuration in calculation.

OCIS codes: 220.0220, 230.3720.

1. Introduction

Recently, many studies have been performed with a view to improving the optical properties in the liquid crystal display (LCD) industry [1–4]. In particular, the rapid growth of the market for mobile devices, such as cell phones and personal digital assistants, has resulted in research that aims to produce high contrast ratios, high brightness, and a wide viewing angle. In this vein, the transflective mode could be an important display mode that can integrate the features of the transmissive mode and the reflective mode. In particular, the current transflective liquid crystal (LC) mode emphasizes higher brightness in addition to a wide viewing angle and high contrast ratio because the high resolution of the display can deteriorate the brightness of the cell. Therefore, this research will apply a circular polarizer, rather than a linear polarizer, to the current outdoor display because of its high brightness. To demonstrate the good electro-optical characteristics of the transflective mode using a circular polarizer, several pieces of research have been studied that looked at improving the optical configuration of the LC cell. For example, Ko *et al.* showed an optical configuration using a biaxial film and a *C*-plate for the reflective mode in order to improve optical characteristics [5]. A combination of an *A*-plate and a *C*-plate was proposed by Chen *et al.* [6], and a combination of two *A*-plates, a *C*-plate, and a biaxial film was proposed by Ge *et al.* [7]. Hong *et al.* [8] proposed an optical configuration

0003-6935/10/203875-08$15.00/0

consisting of two C-plates and two A-plates in order to reduce the off-axis light leakage in the dark state. However, these researchers considered the optimization of the cell at only a single wavelength, so they did not discuss the wideband property.

Another optical configuration, proposed by Pancharatnam [9], conceptually applied the wideband property by using the combination of a uniaxial $\lambda/2$ plate and a uniaxial $\lambda/4$ plate [10], so that it could expect an excellent dark state in the normal direction. However, the proposed optical configuration did not consider optical performance in an oblique direction, so that it could not show a good viewing angle property.

To satisfy the both the wideband and wide viewing angle requirements for the transflective mode, therefore, in this paper we propose an optical configuration that can provide a good optical property for the wideband and a wide viewing angle for a vertical alignment (VA) LCD. We expect that the wideband property will be attained using a wideband $\lambda/4$ plate that consists of a $\lambda/2$ biaxial film and a uniaxial $\lambda/4$ plate. Moreover, we also expect a wide viewing angle property owing to the $\lambda/2$ biaxial film and an additional negative C-plate. The optimization of the optical films used has been performed on the Poincaré sphere in the entire visible wavelength using the Stokes vector and the Mueller matrix method. We compared the optical characteristics of the proposed optical configuration with the conventional mode, which uses a combination of a $\lambda/2$ uniaxial film and a uniaxial $\lambda/4$ plate for the wideband property in the normal direction, in calculations for the verification of the proposed configuration.

2. Off-Axis Light Leakage of the Conventional Circular Polarizer in the Dark State

A. Off-Axis Light Leakage in the Dark State

In general, there are several reasons for the light leakage of an LCD in an oblique direction. One can be the shift of the polarization axis of the polarizer and the optical axis in each optical film. This causes a change in the effective principle axis of the optical films as a function of the observation direction (the polar angle θ and the azimuth angle φ) by the deviation angle δ [11]. The second reason is the change in the retardation value of the compensation film in the oblique incidence. The change of retardation value Γ in each optical film as functions of the polar θ and the azimuth angle φ of the incident light can be easily calculated using the extended 2×2 Jones matrix method [12–14]. The last factor is the dispersion of the refractive index of the optical films along the wavelength [15,16]. The polarization states of the three primary colors (red, green, and blue) commonly differ from one another after passing through the LC cell and the compensation films, due to their dissimilar material and wavelength dispersion properties. Thus, in order to achieve an excellent dark state at the oblique incidence, the phase dispersion in the entire visible wavelength should be removed.

B. Polarization States in the Reflective Mode

The conventional configuration of the transflective circular polarizer comprises two linear polarizers, four positive A-plates and the VA LC cell, as shown in Fig. 1(a). In this paper, we assume that the optical axis of the VA LC cell in the absence of an electric field can be the same as the optical axis of the positive C-plate. Figure 1(b) represents the polarization states for the reflective mode on the Poincaré sphere when the light passes through the cell in the normal direction. The symbols ◆, ■, and • separately express the polarization state of the light with blue ($b = 450$ nm), green ($g = 550$ nm), and red wavelengths ($r = 630$ nm). The starting position is at position T, where the ambient light passes normally through the upper linear polarizer. Then, after passing through the two upper positive A-plates and the VA LC cell, the polarization states of the light move to positions C_r, C_g, and C_b. The position C, which has a circular polarization, is converted to position A after passing through the reflector surface, VA LC layer, and two upper positive A-plates. This means that the conventional circular polarizer shows a perfect dark state at normal incidence. However, the reflective mode of the conventional circular polarizer exhibits a large amount of off-axis light leakage. Figure 1(c) illustrates the change in the polarization state for an oblique incident light inside the conventional circular polarizer for the diagonal direction. In the dark state, the oblique incident light is affected by the deviated angle δ compared to the normal incidence, when it passes the upper linear polarizer. Thus, the polarization position of the transmission axis of the upper linear polarizer deviates by 2δ from S_1 on the Poincaré sphere. Therefore, the starting polarization position at the oblique incidence is position T. The polarization positions of the light after passing through the upper $\lambda/2$ and $\lambda/4$ positive A-plates move to position C owing to the off-axis phase retardation of the two positive A-plates. Then, the polarization positions D_r, D_g, and D_b after the light passes through the $\lambda/4$ VA-cell with a fast axis Q is fairly different from position $-S_3$. Here, we can see that the large difference between positions D_r, D_g, and D_b and position $-S_3$ will induce serious off-axis light leakage in the dark state.

C. Polarization States in the Transmissive Mode

Figure 1(d) depicts the polarization state on the Poincaré sphere when light passes through the transmissive mode from the lower linear polarizer in a normal direction. On the Poincaré sphere, the transmission axis of the lower linear polarizer is represented by the position T, while position A represents the absorption axis of the upper linear polarizer. Positions A and T correspond with each other when the upper and lower linear polarizers are crossed. The start position in the normal incidence is position T when the

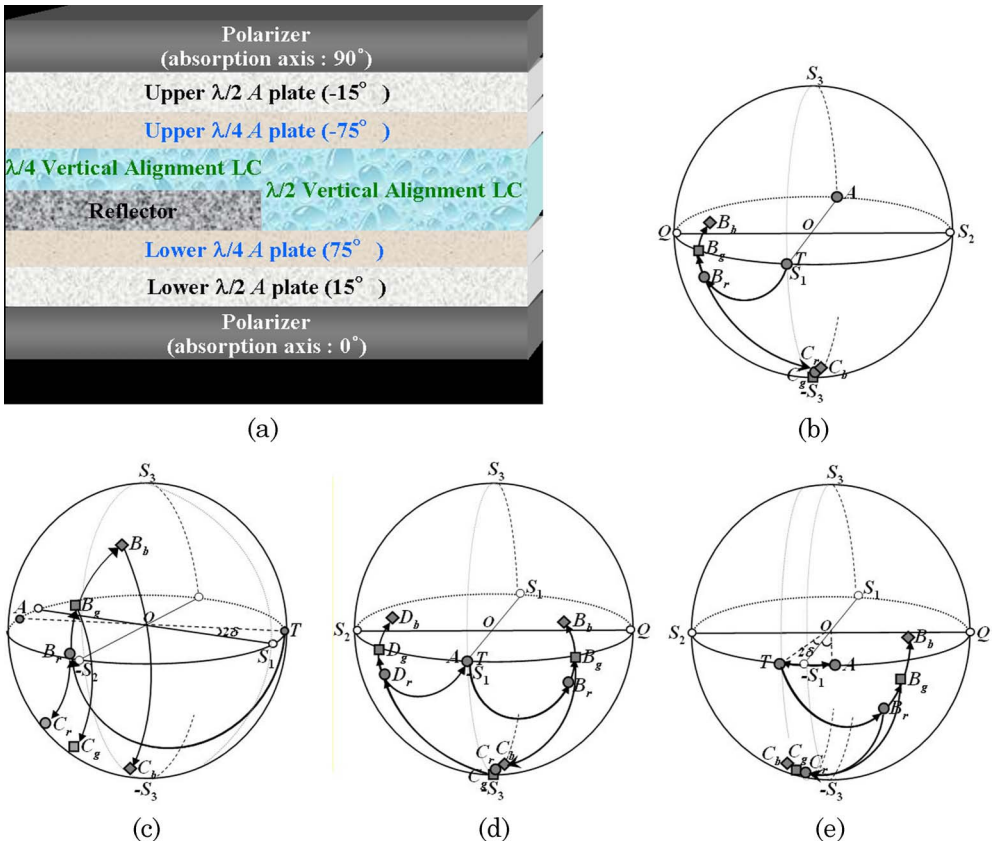

Fig. 1. (Color online) Optical configuration and polarization states of the conventional configuration: (a) optical structure; (b) polarization path on the Poincaré sphere for R-mode in the normal direction and (c) in the diagonal direction; (d) polarization path on the Poincaré sphere for T-mode in the normal direction and (e) in the diagonal direction.

light passes through the lower linear polarizer. Then, the polarization states of the light after passing through the lower $\lambda/2$ positive A-plate are positions B_r, B_g, and D_b. The polarization positions of the light change from B_r, B_g, and B_b to C_r, C_g, and C_b after passing through the lower $\lambda/4$ positive A-plate. In the same way, position C, which has a circular polarization, will be converted to position A after passing through the upper $\lambda/4$ and $\lambda/2$ positive A-plates. Thus, an excellent dark state can be obtained in the normal incidence. However, the conventional circular polarizer for the transmissive mode also exhibits light leakage in the oblique incidence. Figure 1(e) shows the polarization state when the light obliquely passes through the cell in a diagonal direction ($\theta = 70°$ and $\varphi = 45°$). The start position on the Poincaré sphere is position T when the light obliquely passes through the lower linear polarizer. Then, the polarization positions C_r, C_g, and C_b after passing through the lower $\lambda/2$ and $\lambda/4$ positive A-plates deviate from circle S_1–S_3 due to the accumulation of off-axis phase retardation from the lower positive A-plates. Thus, we can observe that light leakage occurs in the oblique incidence because the final polarization position of the light passing through the optical components in front of the final polarizer can be quite different from the polarization position of the absorption axis of the upper linear polarizer.

3. Advanced Optical Configuration Using the $\lambda/2$ Biaxial Film and the Negative *C*-Plate for the Transflective Circular Polarizer

A. Polarization States and Optimization of Optical Films in the Reflective Mode

To minimize light leakage at the oblique incidence, we propose to use $\lambda/2$ biaxial film instead of uniaxial $\lambda/2$ film and a negative C-plate, as shown in Fig. 2(a). Figure 2(b) represents the change of the polarization state for the reflective mode on the Poincaré sphere when the light passes through the proposed configuration in the diagonal direction. The start position is position T, when the light passes obliquely through the upper linear polarizer. Then, the polarization position of the light changes from T to B after passing through the upper $\lambda/2$ biaxial film. The polarization position B moves to position D after passing through the upper $\lambda/4$ positive A-plate and the upper negative C-plate. Then, the polarization position of the light moves to position E in front of the reflector after passing through the $\lambda/4$ VA-cell. Finally, after passing through the reflector, the polarization position of the light is converted to position A, having passed through the $\lambda/4$ VA cell, the upper negative C-plate, the upper $\lambda/4$ positive A-plate, and the upper $\lambda/2$ biaxial film. Thus, a perfect dark state can be obtained in the oblique incidence. To change the

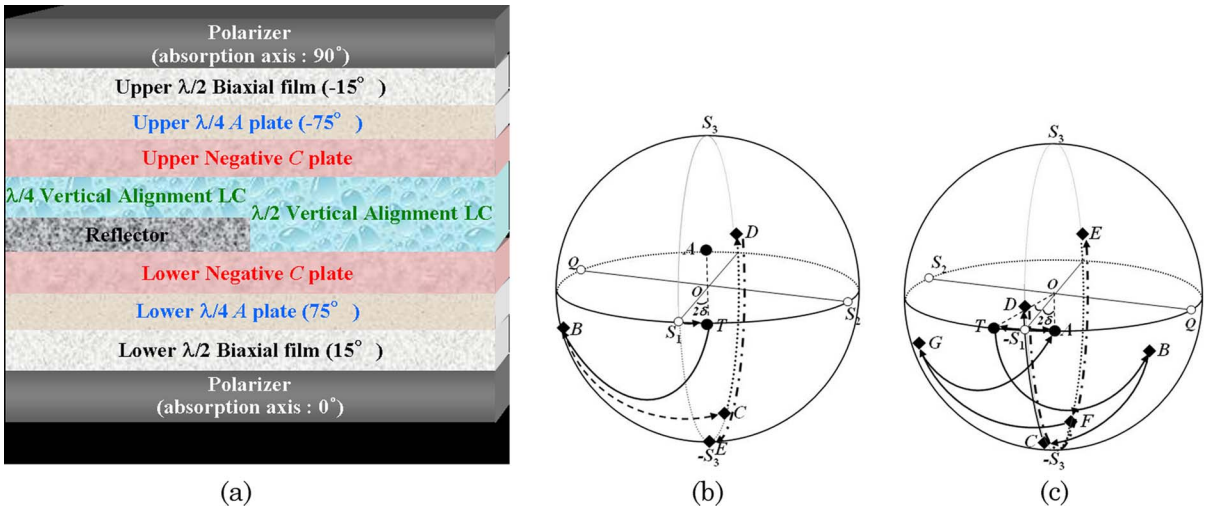

Fig. 2. (Color online) Optical configuration and polarization states of the proposed configuration: (a) optical structure, (b) polarization path on the Poincaré sphere for R-mode in the diagonal direction, and (c) polarization path on the Poincaré sphere for T-mode in the diagonal direction.

polarization position of the light in front of the reflector at the $-S_3$ position in the oblique incidence, the following two conditions for the polarization state of the light in Fig. 2(b) should be satisfied. The first condition is that, after passing through the upper $\lambda/2$ biaxial film and the upper $\lambda/4$ positive A-plate, the polarization positions of the r, g, and b wavelengths should be on the circle S_1–S_3, as shown in Fig. 2(b). For the calculation, we assume that the upper $\lambda/4$ positive A-plate has a normal wavelength dispersion, in which retardation decreases in proportion to an increase in wavelength. The optical configuration is optimized in the diagonal direction ($\theta = 70°$ and $\varphi = 45°$) because the off-axis light leakage can be maximized under this condition [9]. To satisfy the first condition, we calculate the polarization position of the light as a function of parameter $N_z[= (n_x - n_z)/(n_x - n_y)]$ after the light passes through the upper $\lambda/2$ biaxial film and the upper $\lambda/4$ positive A-plate. When the N_z factor of the upper $\lambda/2$ biaxial film changes from 0 to 0.8, the polarization position of the light changes after passing through the upper $\lambda/2$ biaxial film and the upper $\lambda/4$ positive A-plate, as shown in Fig. 3(a). Here, the arc length is dependent on its in-plane phase retardation value $d(n_x - n_y)$, where d is the thickness and $(n_x - n_y)$ is the in-plane birefringence of the upper $\lambda/2$ biaxial film. These parameters should be considered to ensure that the polarization position moves to circle S_1–S_3. From the calculated result, we confirmed that the first condition for compensating for the oblique incidence can be satisfied with an upper $\lambda/2$ biaxial film with $N_z \approx 0.36$. The second condition is the determination of the retardation value of the upper negative C-plate.

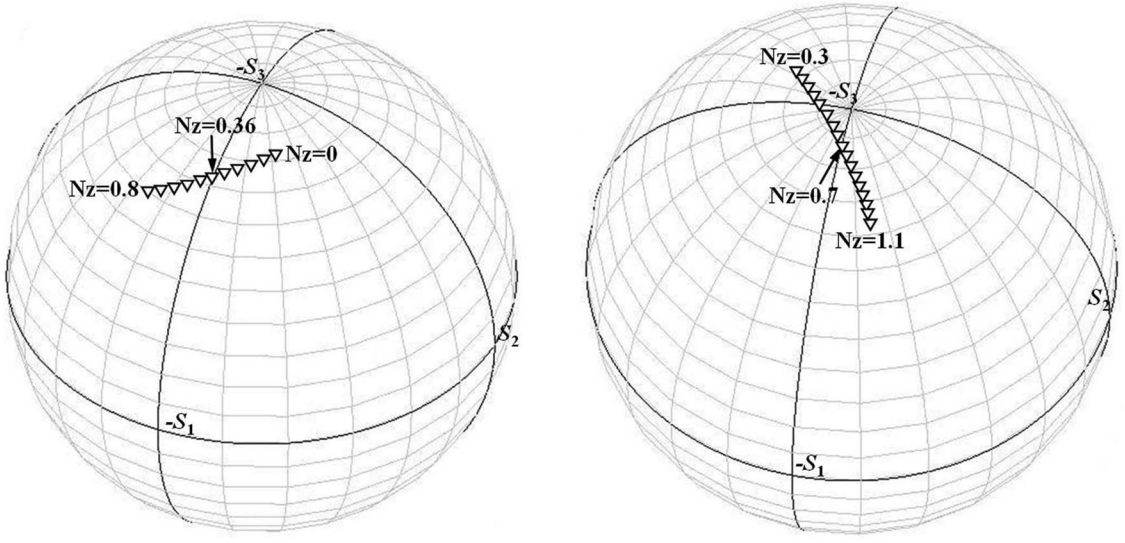

Fig. 3. Polarization distribution of the light after passing through the $\lambda/2$ biaxial film and the $\lambda/4$ positive A-plate as a function of N_z factor: (a) for R-mode and (b) for T-mode.

Table 1. Calculated Optimized Dispersion Properties of the Optical Anisotropy of the Optical Uniaxial Films

	$\Delta n/\Delta n$ (550 nm)		Δnd (nm)
	450 nm	630 nm	550 nm
Upper positive A-plate	1.016	0.978	128
Upper negative C-plate	1.132	0.992	−231
Lower positive A-plate	1.005	0.978	128
Lower negative C-plate	1.021	0.948	−295

Here, we can easily calculate the retardation value of the negative C-plate by using the Mueller matrix and the Stokes vector [17,18]. The four Stokes parameters can usually be written as

$$S = (S_0, S_1, S_2, S_3)^T. \tag{1}$$

The Stokes parameters for the three primary wavelengths of light that have passed through the upper negative C-plate can be described as follows:

$$\begin{aligned} S' &= R(-2\theta)\cdot M(\Gamma)\cdot R(2\theta)\cdot S(A+) \\ &= \begin{pmatrix} 1 & 0 & 0 & 0 \\ 0 & \cos^2 2\theta + \cos\Gamma \sin^2 2\theta & (1-\cos\Gamma)\sin 2\theta \cos 2\theta & \sin\Gamma \sin 2\theta \\ 0 & (1-\cos\Gamma)\sin 2\theta \cos 2\theta & \sin^2 2\theta + \cos\Gamma \cos^2 2\theta & -\sin\Gamma \cos 2\theta \\ 0 & \sin\Gamma \sin 2\theta & \sin\Gamma \cos 2\theta & \cos\Gamma \end{pmatrix} \begin{pmatrix} S_{0A+} \\ S_{1A+} \\ S_{2A+} \\ S_{3A+} \end{pmatrix} = \begin{pmatrix} S_0' \\ S_1' \\ S_2' \\ S_3' \end{pmatrix}, \end{aligned} \tag{2}$$

where $R(2\theta)$ and $R(-2\theta)$ are the rotating matrix and reverse rotating matrix to the principal axis. $M(\Gamma)$ depicts the Mueller matrix for rotated polarizing components with phase retardation Γ. $S(A+)$ is the Stokes vector of the incident light after passing through the upper $\lambda/4$ positive A-plate, and S' represents the Stokes vector of the output light. S_{0A+}, S_{1A+}, S_{2A+}, and S_{3A+} are the Stokes polarization parameters of the Stokes vector $S(A+)$.

To move the polarization position of the light after it has passed through the $\lambda/4$ VA-cell to the position $-S_3$, the polarization position of light that has passed through the upper negative C-plate, for the three primary wavelengths, should be located in the position D, as shown in Fig. 2(b). Here, the Stokes vector of position D is $(1, -0.99239, -0.00224, 0.123066)^T$, so we can obtain the retardation value of the negative C-plate by using Eq. (2).

Table 2. Calculated Optimized Dispersion Properties of the Optical Anisotropy of the Optical Biaxial Films

	$\Delta n/\Delta n$ (550 nm) ($\Delta n = n_x - n_y - n_z - n_y$)		Δnd (nm) $\Delta n = n_x - n_y$)
	450 nm	630 nm	550 nm
Two biaxial films	1.004	0.996	256

B. Polarization States and Optimization of Optical Films in the Transmissive Mode

Figure 2(c) depicts the change in the polarization state for the transmissive mode on the Poincaré sphere when the light passes through the proposed configuration in the diagonal direction. The starting position is at position T when the light passes obliquely through the lower linear polarizer. Then, the polarization position of the light changes from T to B after passing through the lower $\lambda/2$ biaxial film. The polarization position moves to position D after passing through the lower $\lambda/4$ positive A-plate and the lower negative C-plate. Then, the polarization position of the light moves to position F after passing through the $\lambda/2$ VA-cell and the upper negative C-plate. Finally, the polarization position is converted to position A due to the upper $\lambda/4$ positive A-plate and the upper $\lambda/2$ biaxial film ($N_z \approx 0.36$). Therefore, the off-axis light leakage is eliminated in the oblique incidence because position A overlaps the absorption axis orientation of the upper linear polarizer, as shown in Fig. 2(c). Here, we need to satisfy two conditions to gather the polarization positions of the entire visible wavelength to position A. Like the reflective mode, the first condition is that, after passing through the lower $\lambda/2$ biaxial film and the lower $\lambda/4$ positive A-plate, the polarization positions for the r, g, and b wavelengths should be on the circle S_1–S_3, as shown in Fig. 2(c). For the calculation, we assume that the lower $\lambda/4$ positive A-plate has normal wavelength dispersion. To satisfy the first condition, we calculate the polarization position of the light as a function of parameter N_z after light passes through the lower $\lambda/2$ biaxial film and the lower $\lambda/4$ positive A-plate. When the N_z factor of the lower $\lambda/2$ biaxial film changes from 0.3 to 1.1, the polarization position of the light after passing through the lower $\lambda/2$ biaxial film and the lower $\lambda/4$ positive A-plate changes, as shown in Fig. 3(b). From the calculated result, we confirmed that the first condition for compensation for the oblique incidence can be satisfied with a lower $\lambda/2$ biaxial film with $N_z \approx 0.7$. The second condition for optimization is to determine the retardation value of the lower negative C-plate. To move the final polarization position to position A, the polarization position of the light after passing through the lower negative C-plate in the entire visible wavelength should coincide with position D, as shown in Fig. 2(c).

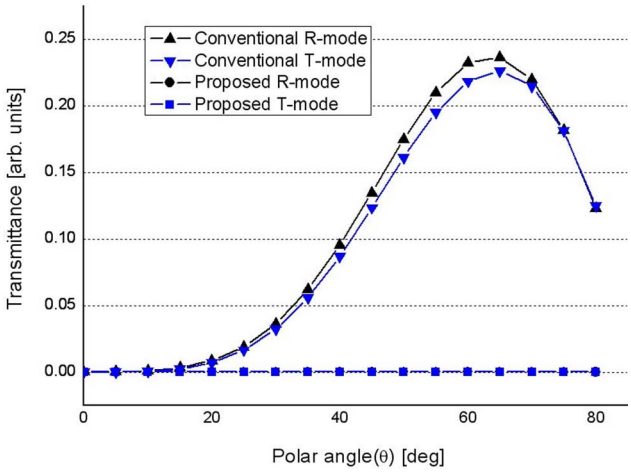

Fig. 4. (Color online) Comparison of the optical transmittance between the conventional and the proposed configuration as a function of the polar angle at $\varphi = 45°$ in the dark state.

Here, the Stokes vector of position D is $(1, -0.98986, -0.00114, 0.14201)^T$, so we can easily calculate the retardation value of the lower negative C-plate by using Eq. (2).

Tables 1 and 2 show the calculated optimized retardation values of the compensation films used for the r, g, and b wavelengths. In this calculation, we set the dispersion property of the VA LC as $\Delta n(\lambda = 450\ \text{nm})/\Delta n(\lambda = 550\ \text{nm}) = 104$ and $\Delta n(\lambda = 630\ \text{nm})/\Delta n(\lambda = 550\ \text{nm}) = 0.98$. The cell gap d was set to 3.8 and 7.6 μm for the calculation. With respect to the material dispersion, we can see that both the $\lambda/2$ biaxial film and the negative C-plate should have a normal dispersion property to gain an achromatic dark state. We compared the optical transmittance of the proposed circular polarizer with that of the conventional circular polarizer for the dark state, as shown in Fig. 4. We can observe that the proposed configuration effectively removes the off-axis light leakage in the dark state. We verified the improved viewing angle of the proposed configuration by using the commercial LC software TechWiz LCD provided

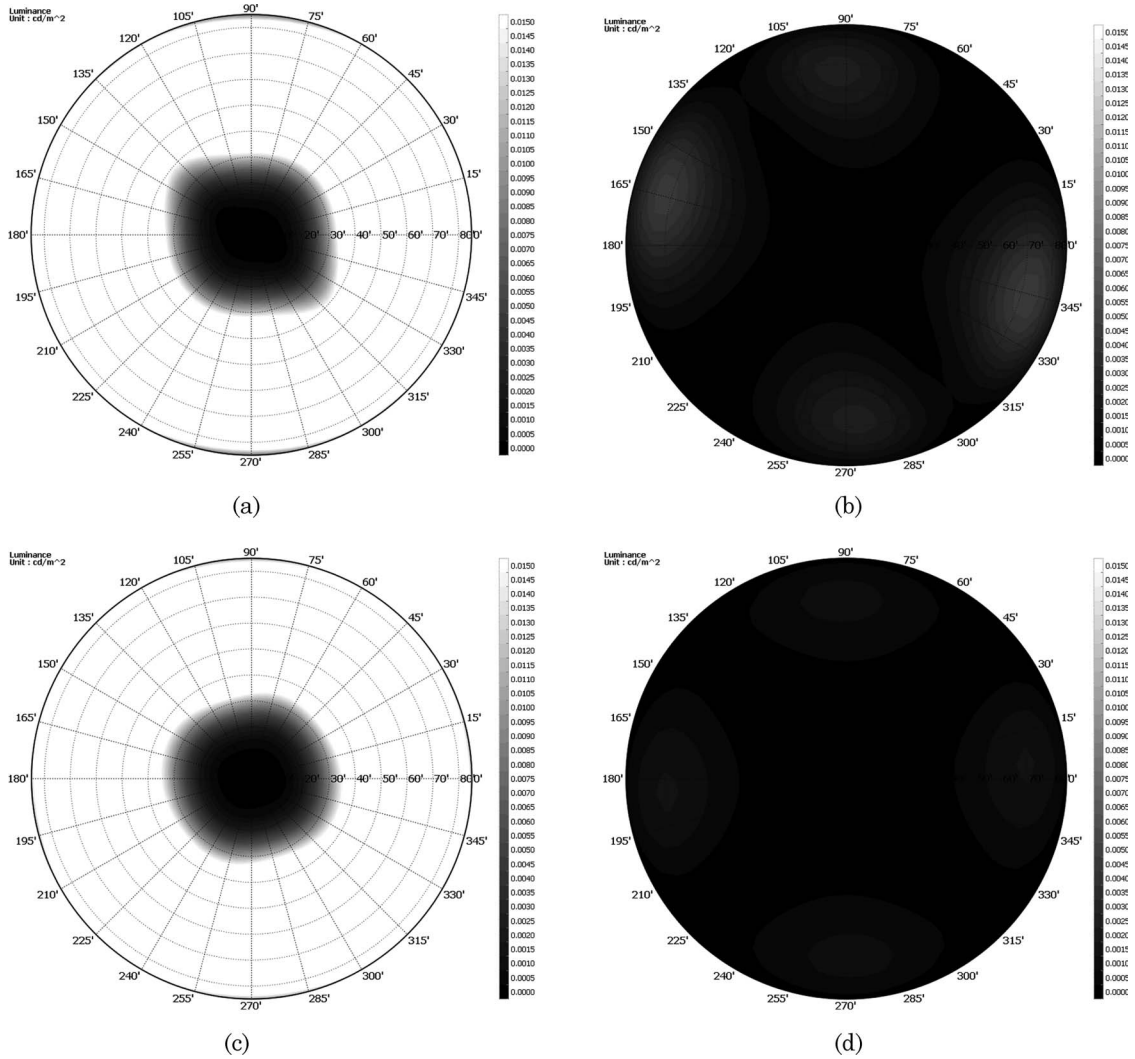

Fig. 5. Calculated luminance in the dark state: (a) the conventional configuration for R-mode and (b) the proposed configuration for R-mode, and (c) the conventional configuration for T-mode and (d) the proposed configuration for T-mode.

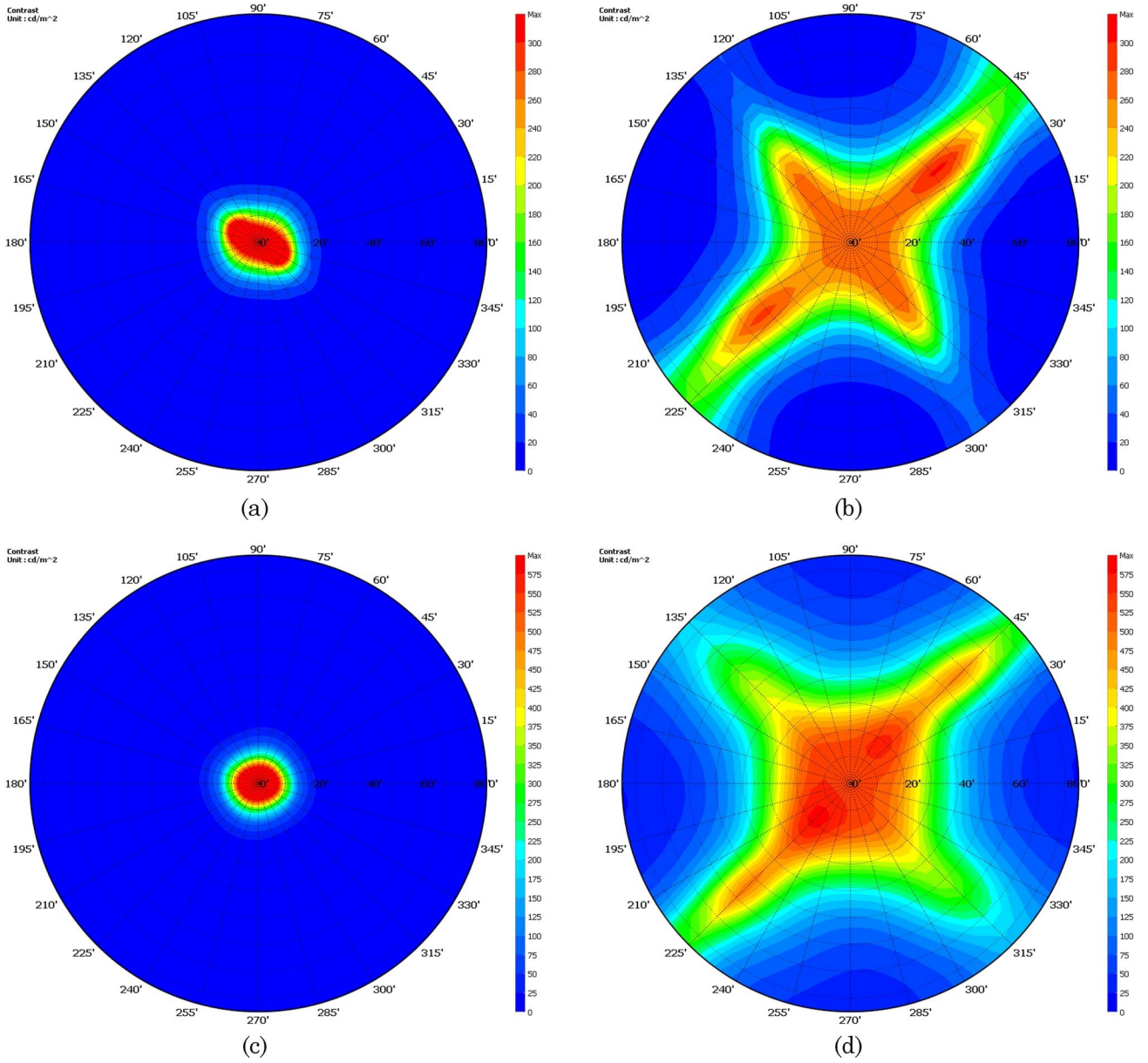

Fig. 6. (Color online) Calculated isocontrast contour: (a) the conventional configuration for R-mode and (b) the proposed configuration for R-mode, and (c) the conventional configuration for T-mode and (d) the proposed configuration for T-mode.

by the Sanayi System Co. in Korea instead of performing experiments, because each optimized film takes a very long time to be supported. Figure 5 shows the comparison of the luminance of the proposed configuration with that of the conventional configuration in the dark state. Figure 6 compares the normalized isocontrast contour of the conventional configuration with that of the proposed configuration in the visible wavelength range. From the calculated results in Figs. 5 and 6, we proved that the proposed configuration has a higher contrast ratio than the conventional configuration, as it reduces the off-axis light leakage in the dark state.

4. Conclusions

In this study, we demonstrated a high contrast ratio circular polarizer with wideband and wide viewing angle properties using a $\lambda/2$ biaxial film and negative C-plate. To eliminate off-axis light leakage in the dark state and to obtain an excellent dark state, we augmented the compensation films used for phase dispersion of the entire visible wavelength range using the Stokes vector and the Mueller matrix on the Poincaré sphere. From numerical calculations, the proposed configuration is shown to have wide viewing angle and high contrast ratio characteristics due to compensating for light leakage in the diagonal direction. Thus, we believe that the proposed circular polarizer will suffice for mobile display applications in transflective LCD technologies.

This work was supported by Samsung Mobile Display.

References

1. Y. Yamaguchi, T. Miyashita, and T. Uchida, "Wide-viewing-angle display mode for the active-matrix LCD using bend-alignment liquid-crystal cell," in *Society for Information Display 1993 Digest* (1993), pp. 277–280.
2. M. Oh-e and K. Kondo, "Electro-optical characteristics and switching behavior of the in-plane switching mode," Appl. Phys. Lett. **67**, 3895–3897 (1995).
3. S. H. Lee, S. L. Lee, and H. Y. Kim, "Electro-optic characteristics and switching principle of a nematic liquid crystal cell controlled by fringe-field switching," Appl. Phys. Lett. **73**, 2881–2883 (1998).
4. K. H. Kim, K. Lee, S. B. Park, J. K. Song, S. N. Kim, and J. H. Souk, "Domain divided vertical alignment mode with optimized fringe field effect," in *Asia Display '98* (1998), pp. 383–386.
5. T. W. Ko, J. C. Kim, H. C. Choi, K.-H. Park, S. H. Lee, K.-M. Kim, W.-R. Lee, and G.-D. Lee, "Wideband quarter-wave liquid crystal cell with wide viewing angle for the reflective mode with single polarizer," Appl. Phys. Lett. **91**, 053506 (2007).
6. J. Chen, K.-H. Kim, J.-J. Jyu, and J. H. Souk, "Optimum film compensation modes for TN and VA LCDs," in *Society for Information Display 1998 Digest* (1998), pp. 315–318.
7. Z. Ge, R. Lu, T. X. Wu, S.-T. Wu, C.-L. Lin, N.-C. Hsu, W.-Y. Li, and C.-K. Wei, "Extraordinarily wide-view circular polarizers for liquid crystal displays," Opt. Express **16**, 3120–3129 (2008).
8. Q. Hong, T. X. Wu, X. Zhu, R. Lu, and S.-T. Wu, "Extraordinarily high-contrast and wide view liquid-crystal displays," Appl. Phys. Lett. **86**, 121107 (2005).
9. S. Pancharatnam, "Achromatic combinations of birefringent plates," Proc. Math. Sci. **41**, 130–136 (1955).
10. T. H. Yoon, G. D. Lee, and J. C. Kim, "Nontwist quarter-wave liquid-crystal cell for a high-contrast reflective display," Opt. Lett. **25**, 1547–1549 (2000).
11. P. Yeh and C. Gu, *Optics of Liquid Crystal Displays* (Wiley, 1999).
12. A. Lien, "Extended Jones matrix representation for the twisted nematic liquid-crystal display at oblique incidence," Appl. Phys. Lett. **57**, 2767–2769 (1990).
13. X. Zhu, Z. Ge, and S.-T. Wu, "Analytical solutions for uniaxial-film-compensated wide-view liquid crystal displays," J. Display Technol. **2**, 2–20 (2006).
14. D.-K. Yang and S.-T. Wu, *Fundamentals of Liquid Crystal Devices* (Wiley, 2006).
15. Y. Fujimura, T. Kamijo, and H. Yoshimi, "Improvement of optical films for high-performance LCDs," Proc. SPIE **5003**, 96–105 (2003).
16. J.-H. Lee, H. C. Choi, S. H. Lee, J. C. Kim, and G. D. Lee, "Optical configuration of a horizontal-switching liquid-crystal cell for improvement of the viewing angle," Appl. Opt. **45**, 7279–7285 (2006).
17. J. E. Bigelow and R. A. Kashnow, "Poincaré sphere analysis of liquid crystal optics," Appl. Opt. **16**, 2090–2096 (1977).
18. K. Vermeirsch, A. D. Meyere, J. Fornier, and H. D. Vleeschouwer, "Viewing angle of liquid-crystal displays: representation on the Poincaré sphere," Appl. Opt. **38**, 2775–2786 (1999).